Glass Transition

U. Buchenau

This document has been published in

Manuel Angst, Thomas Brückel, Dieter Richter, Reiner Zorn (Eds.):
Scattering Methods for Condensed Matter Research: Towards Novel Applications at Future Sources
Lecture Notes of the 43rd IFF Spring School 2012
Schriften des Forschungszentrums Jülich / Reihe Schlüsseltechnologien / Key Technologies, Vol. 33
JCNS, PGI, ICS, IAS
Forschungszentrum Jülich GmbH, JCNS, PGI, ICS, IAS, 2012
ISBN: 978-3-89336-759-7

E 9 Glass Transition

U. Buchenau
Institut für Festkörperforschung
Forschungszentrum Jülich GmbH

Contents

[0]Lecture Notes of the 43^{rd} IFF Spring School "Scattering Methods for Condensed Matter Research: Towards Novel Applications at Future Sources" (Forschungszentrum Jülich, 2012).

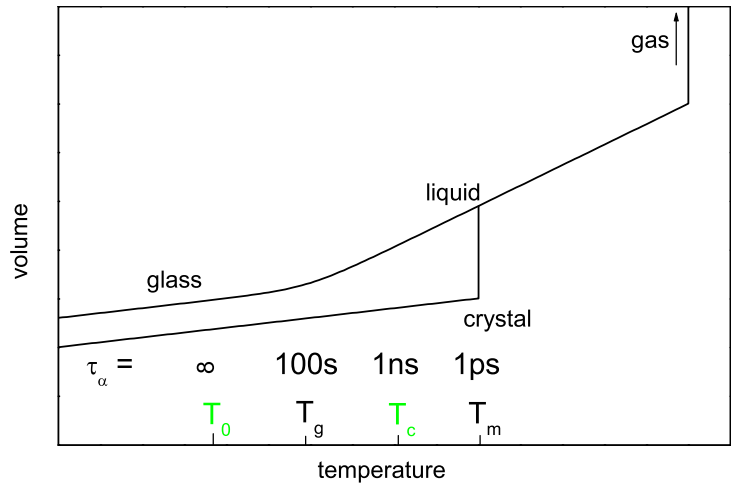

Fig. 1: *Volume-temperature diagram of the crystalline, glassy and liquid phase at ambient pressure.*

1 Introduction

The glass transition (the freezing of an undercooled and highly viscous liquid into a glass) is considered to be one of the great unsolved riddles of solid state physics. The main riddle is the atomic mechanism of the flow process in the highly viscous liquid and its strong temperature dependence shortly before freezing. The freezing itself is recognized as a falling out of thermal equilibrium, a kinetic process. But it is not clear to which extent this kinetic process reflects a true thermodynamic second order transition at a lower temperature, the Kauzmann or Vogel-Fulcher temperature. The present paper describes the situation of our present knowledge (or lack of knowledge) [1, 2, 3, 4, 5, 6, 7, 8, 9, 10, 11, 12, 13, 14].

Liquids do not crystallize immediately after cooling below their melting points, because the crystallization requires the formation of crystal nuclei, a process which takes time. If this time is long enough to measure the properties of the undercooled liquid at all temperatures, one calls the liquid a glass former. Examples are vitreous silica (one mixes silica with metal oxydes to make window glasses), boron trioxyde, glycerol and selenium. Many polymers are good glass formers, like polystyrene, polycarbonate and polyisoprene (rubber), but others form a mixture of crystalline and amorphous domains like polyethylene.

At the glass transition temperature T_g, the undercooled liquid freezes into a glass, a solid with a nonzero shear rigidity. In many liquids, this glass temperature is about 2/3 of the melting temperature. From numerical simulation results (to be discussed in more detail in Section 4 on new developments), we now believe that every liquid can be cooled into a glass, provided the cooling rate is high enough. However, in real liquid water it is impossible to carry the heat fast enough away, so it can only be frozen into the glass state on the computer.

In undercooled liquids, the viscosity increases drastically with decreasing temperature. This increase reflects the dramatic increase of the structural relaxation time τ_α of the liquid (it is denoted by α to distinguish it from possible secondary relaxations β, γ etc. at lower temperatures in the glass phase). The structural α-relaxation is visible not only in mechanical, but also in dielectric, light scattering or heat capacity spectra. The glass transition occurs for a relaxation time of about 100 seconds.

Fig. 1 shows the cooling process from the gas phase into the liquid phase and then into the glass

phase in a volume-temperature diagram at ambient pressure. There is a large volume jump between gas and liquid, much larger than the volume jump at the first order phase transition between liquid and crystal at T_m. If the crystallization is avoided by fast enough cooling, the system enters the undercooled liquid and experiences the drastic slowing down of the relaxation time τ_α with decreasing temperature indicated in the figure. The glass temperature T_g depends on the cooling rate R according to

$$\tau_\alpha(T_g) \approx T_g/R, \tag{1}$$

because T_g/R is roughly the time needed to cool the whole energy of the sample away. So the faster the cooling, the higher is T_g. For a glass temperature of 200 K, a cooling rate of 1 K/s implies a τ_α of 200 s. As will be seen in the next section, τ_α is only a mean of a broad distribution of relaxation times, which makes the glass transition even more diffuse in temperature.

The thermal expansion of the glass is similar to the one of the crystal. It is due to the anharmonicity of the vibrations [1]. The thermal expansion of the liquid phase is a factor of two to four higher than the one of the glass phase (there is one important exception, vitreous silica, which will be discussed below).

From the theoretical understanding, there are two other important temperatures shown in Fig. 1. The first is the Vogel-Fulcher temperature T_0 below T_g where the viscosity and τ_α extrapolate to infinity. As will be seen, the Vogel-Fulcher temperature lies close to the Kauzmann temperature T_K, where the structural entropy of the liquid extrapolates to zero. This will be discussed in more detail in the next two sections. The second theoretical temperature, T_c, lies between T_g and T_m and is the critical temperature of the mode coupling theory [3]. The mode coupling theory is the most advanced liquid theory up to day. According to this theory, the viscosity should diverge at the critical temperature T_c. Therefore one has to invoke additional thermally activated hopping processes to explain why the real viscosity is still small at this temperature. A very recent theoretical treatment in terms of the replica technique [15] shows that T_c is the point in temperature where it becomes possible to measure a limiting shear modulus G_{high} for high enough frequency (G_{high} is sometimes denoted by G_∞, but this term should be reserved for the shear modulus of an instantaneous affine shear deformation [8]). From an empirical energy landscape point of view [5], T_c is the temperature below which one can distinguish between the fast picosecond relaxation processes and the slow thermally activated α-relaxation of the flow process close to the Maxwell time τ_M

$$\tau_\alpha \approx \tau_M = \frac{\eta}{G_{high}}, \tag{2}$$

where η is the viscosity. Since G_{high} is of the order of GPa, a viscosity of 10^{12} Pa s implies a Maxwell time of 1000 s.

The scattering methods discussed in the present spring school are of central importance for the study of the glass transition. Naturally, their time resolution is not good enough to study the α-process itself close to T_g, but they supply other essential information. This is illustrated in Fig. 2, which shows the mean square displacement of crystalline, glassy and liquid selenium as a function of temperature. There is a close parallel to Fig. 1, because the mean square displacement of the undercooled liquid, together with the anharmonicity of the interatomic potential, supplies the physical reason for the thermal expansion [1]. One realizes immediately that the understanding of the undercooled liquid requires a study of the atomic motion on the fast picosecond scale.

In a crystal, the simplest approximation relates the mean square displacement to a mean atomic frequency, the Debye frequency ω_D. If the temperature is high enough, one can use the classical

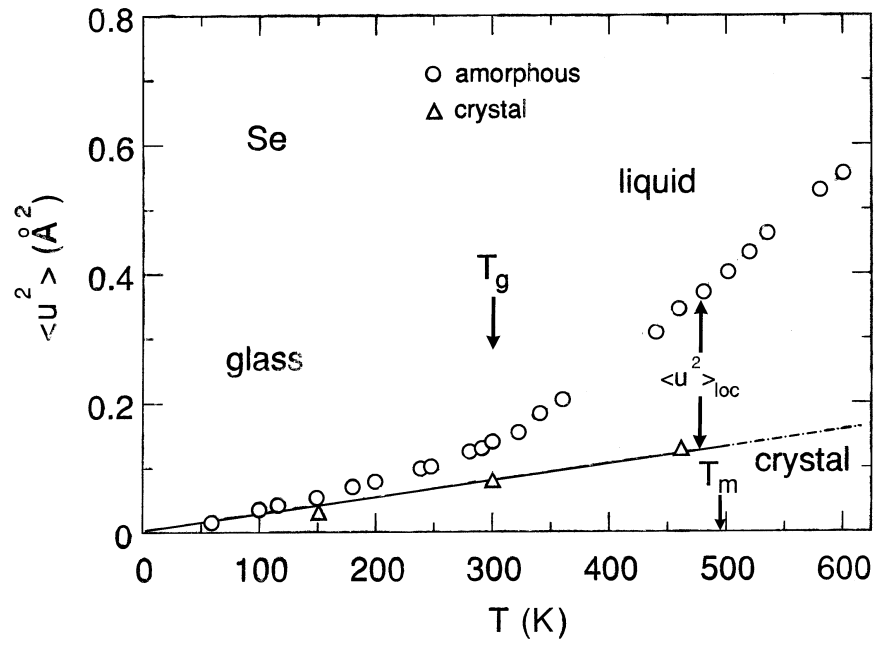

Fig. 2: *Mean square atomic displacements in crystalline, glassy and liquid selenium [16].*

approximation

$$< u^2 >= \frac{3k_BT}{M\omega_D^2}, \tag{3}$$

where M is the average atomic mass. In the simplest case of elastic isotropy, the Debye frequency is determined by the density ρ and the longitudinal and transverse sound velocities v_l and v_t, respectively

$$\omega_D^3 = \frac{18\pi^2\rho}{M(1/\mathrm{v}_l^3 + 2/\mathrm{v}_t^3)}. \tag{4}$$

In turn, the longitudinal and transverse sound velocities are related to the two elastic constants of the isotropic medium, the bulk modulus B_{high} and the shear modulus G_{high} by

$$\rho\mathrm{v}_l^2 = B_{high} + \frac{4}{3}G_{high} \qquad \rho\mathrm{v}_t^2 = G_{high}, \tag{5}$$

where the index $high$ indicates the elastic constant for high frequency and is not necessary in a solid. In a liquid, one has to make the distinction, because even the bulk modulus is markedly higher at high frequency.

The question is whether the simple description in terms of elastic constants still makes sense in a complicated glass former. This question can be answered by inelastic neutron scattering experiments, which are able to measure the vibrational density of states and its temperature dependence. It is this temperature dependence which is responsible for the strong rise of $< u^2 >$ in Fig. 2. It has been measured by Wuttke et al [17] in glycerol, a molecular glass former which exhibits the same $< u^2 >$-behavior as selenium and where the temperature dependence of the high-frequency elastic constants has also been measured [18]. The temperature dependence of the neutron spectra is shown in Fig. 3. The spectra are evaluated in terms of the vibrational

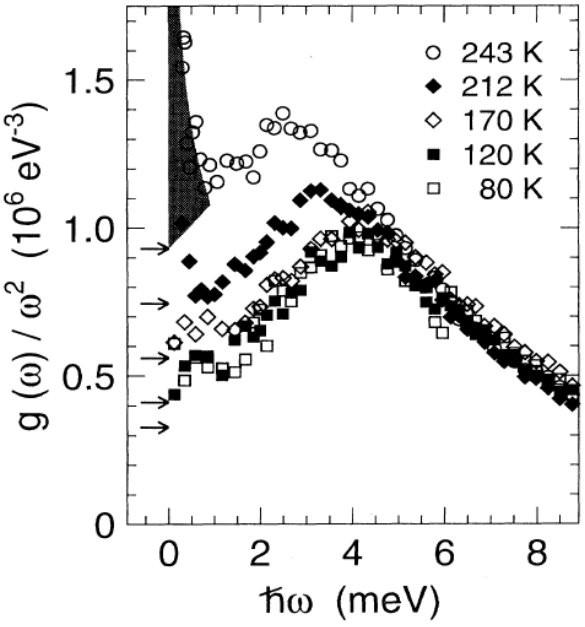

Fig. 3: *Measured spectra [17] in glycerol above and below its glass temperature T_g = 190 K, plotted as $g(\omega)/\omega^2$. The measured curves extrapolate to the arrows denoting the Debye expectation at the different temperatures. At 243 K, one begins to see the tail of the flow or α-process.*

density of states $g(\omega)$ divided by the frequency squared. In this plot, the Debye density of states

$$g_{Debye}(\omega) = \frac{3\omega^2}{\omega_D^3} \tag{6}$$

is a constant which can be calculated from the sound velocities at the given temperature. What one finds, is not a constant, but a broad peak sitting on top of the expected Debye density of states, the so-called boson peak, found universally in all glasses.

The boson peak is another one of the unsolved riddles of disordered matter; it is not clear whether it is due to resonant modes related to the low temperature tunneling states in glasses [19] (and to the plastic modes responsible for the shear thinning [20]) or simply to the force constant disorder in the glass [21]. This peak remains reasonably harmonic in the glass phase (not entirely; one can see some anharmonicity even below T_g), but begins to grow and shift to lower frequency in the undercooled liquid. At 243 K, one begins to see the high frequency tail of the flow process, because it begins to enter the nanosecond range accessible to neutrons, but at lower temperatures the undercooled liquid looks like a hot anharmonic glass in the neutron spectra.

Since the mean square displacement of the atoms is the area under the curve, it begins to grow markedly stronger than proportional to the temperature above T_g, as in Fig. 2. The anharmonicity of the potential is the same in liquid and glass. Therefore the stronger increase of the mean square displacement in the liquid with increasing temperature leads to a stronger thermal expansion [1]. Naturally, the fast vibrations supply only a part (if one analyses it quantitatively [22], only a smaller part, of the order of one quarter) of the additional thermal expansion or of the additional heat capacity in the undercooled liquid; the larger part comes from the slow fluctuations of the flow process at τ_α.

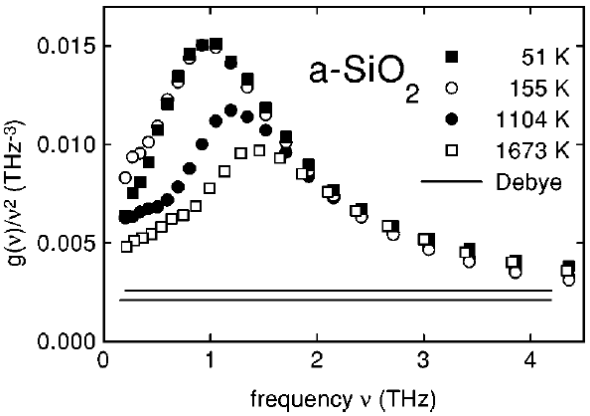

Fig. 4: *Measured spectra [23] in vitreous silica above and below its glass temperature T_g = 1473 K, plotted as $g(\omega)/\omega^2$. The upper line denotes the Debye expectation at 51 K, the lower line at 1673 K.*

As already mentioned above, silica shows an exceptionally different behavior. Fig. 4 shows the measured spectra [23] above and below the glass temperature of 1473 K in silica. One does indeed get the opposite behavior to the normal case in Fig. 3. Instead of growing and lowering its peak frequency, the boson peak decreases and goes to higher frequency with increasing temperature. In fact, one finds a negative thermal expansion below 150 K, where the boson peak vibrations dominate. At higher temperatures, one gets a small positive thermal expansion, because the vibrations at higher frequency have a positive Grüneisen parameter, the normal case [1]. The thermal expansion remains very small up to temperatures above T_g, making silica the closest example for a completely harmonic glass former that has been found so far. We will come back to this point in Section 4.

2 Kinetics of the glass transition

There are two characteristic properties of the kinetics of the α-process (the flow process) in undercooled liquids, the fragility and the stretching. The fragility characterizes the temperature dependence of τ_α and the stretching characterizes the width of the relaxation time distribution.

2.1 Fragility

The usual measure of the fragility of a glass former is the logarithmic slope of the relaxation time τ_α of the flow process

$$m = d\log\tau_\alpha/d(T_g/T)|_{T_g}, \tag{7}$$

in the so-called Angell plot [25] (see Fig. 5) of $\log\tau_\alpha$ as a function of T/T_g at $T/T_g = 1$.
It is useful to relate τ_α to an energy barrier V_α via the Arrhenius relation

$$\tau_\alpha = \tau_0 \exp(V_\alpha/k_B T), \tag{8}$$

where the microscopic attempt frequency is at 10^{-13} s, sixteen decades faster than the flow process at the glass temperature. The *fragility index* I is defined [10] by the logarithmic derivative $I = -d\ln V_\alpha/d\ln T$, taken at T_g. Then

$$m = 16(I+1), \tag{9}$$

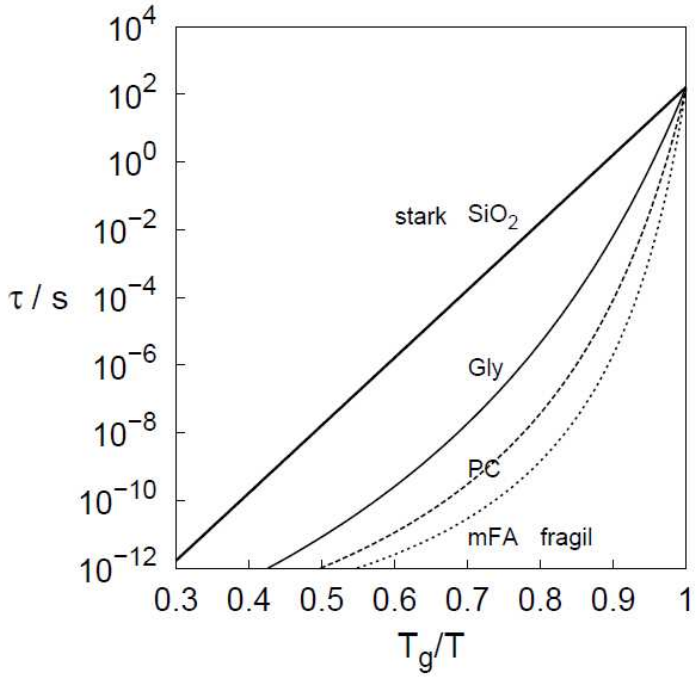

Fig. 5: *The Angell plot shows* $\log \tau_\alpha$ *as a function of* T/T_g*, here for vitreous silica, glycerol and two other glass formers (taken from the thesis of A. Reiser [24]).*

where the factor reflects the sixteen decades between microscopic and macroscopic time scales. I is a better measure of the fragility than m, because it does not contain the trivial temperature dependence of any thermally activated process. If $I = 0$, one has the harmonic case of a temperature-independent energy barrier. Glass formers like vitreous silica with $m = 20$ and $I = 0.25$ are close to this harmonic case and are called strong glass formers, as opposed to to the fragile ones. Glycerol is intermediate with $m = 53$ and $I = 2.3$; the most fragile ones are some polymers with $m = 150$ and $I = 9.4$.
The most popular fitting form for τ_α is the empirical Vogel-Fulcher-Tammann-Hesse relation

$$\log \tau_\alpha = \log \tau_0 + \frac{B}{T - T_0}, \tag{10}$$

which is derived from the Arrhenius equation, eq. (8), by replacing the temperature T in the denominator of the exponent by $T - T_0$. The Vogel-Fulcher temperature T_0 is close to zero in a strong glass and close (but below) T_g in a fragile glass. The Vogel-Fulcher relation predicts a divergence of τ_α at the Vogel-Fulcher temperature. In many glass formers, it equals within the error bars of the experimental determination [26] the thermodynamically defined Kauzmann temperature T_K, suggesting a hidden relation between kinetics and thermodynamics. This will be discussed in more detail in the next section.
Note that the Vogel-Fulcher relation, eq. (10), is known as Williams-Landel-Ferry or WLF-relation in polymers.

2.2 Stretching and dynamical heterogeneity

The second important property of the α-process is its "stretching". The stretching, seen in the time dependence of the α-relaxation, means that there is not only one exponential decay with

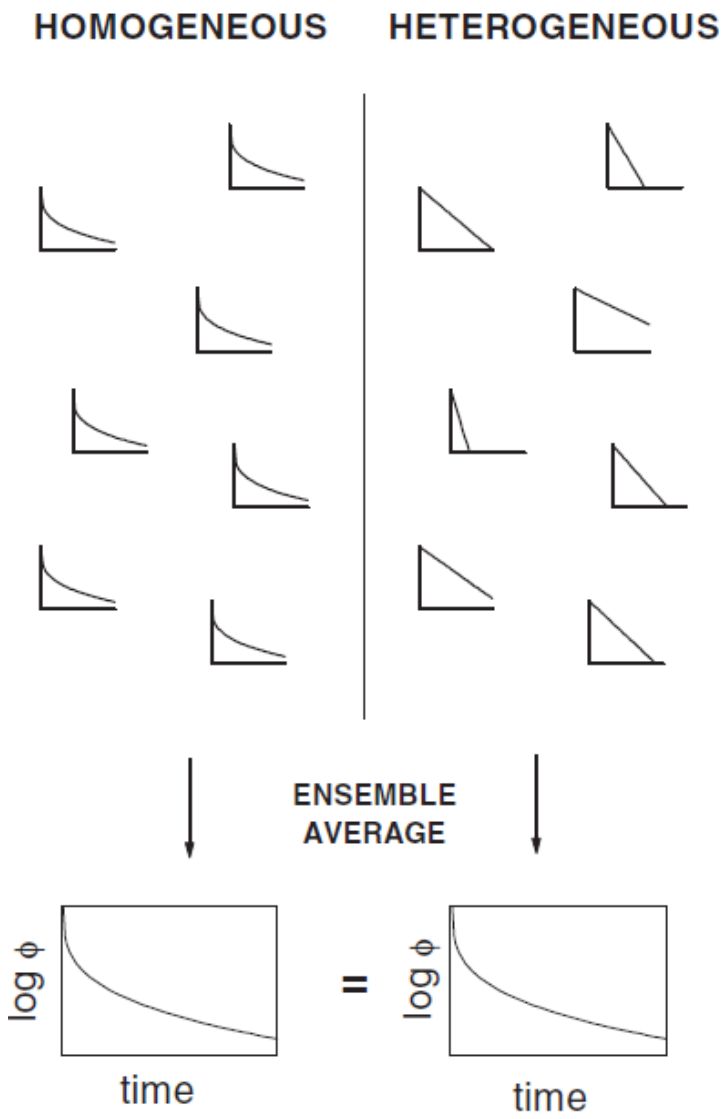

Fig. 6: *The two possible scenarios for the stretching (schematic): On the left dynamical homogeneity, on the right dynamical heterogeneity [28].*

a single relaxation time τ_α, but that one needs a whole distribution of exponential decays with different relaxation times to describe the time dependence of the decay. If one switches on a constant shear strain ϵ_0 in the undercooled sample at the time $t = 0$, the shear stress decay is often well described in terms of a stretched exponential, the so-called Kohlrausch function

$$G(t) = G_{high} \exp(-(t/\tau_\alpha)^\beta). \tag{11}$$

The stretching exponent (the Kohlrausch β) lies between 0.8 and 0.3 (the latter case correspond to a pronounced stretching over three to four decades in time). There is a tendency [27] for a larger stretching for more fragile glass formers, but it is not an exact relation.
If one plots $\log(G(t))$ as a function of time, one sees the stretching in the curvature. $\beta = 1$, the Debye case of a single relaxation time, gives a straight line. The smaller β, the larger the curvature.
The central question with regard to the stretching is whether different regions in the sample have different relaxation times (in this case one talks of dynamical heterogeneity) or whether

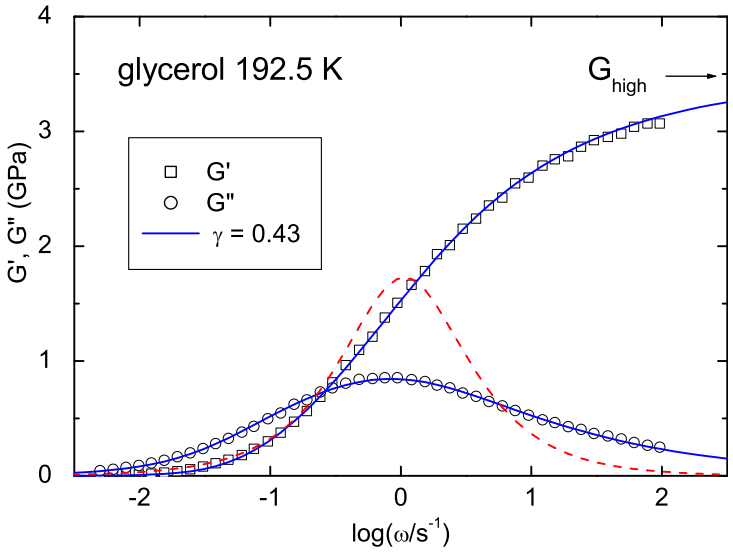

Fig. 7: *Real and imaginary parts $G'(\omega)$ and $G''(\omega)$ of the complex shear modulus in glycerol [29] at 192.5 K as a function of the frequency ω. The continuous line is a fit with a Kohlrausch stretched exponential with $\beta = 0.43$, the dashed line is $G''(\omega)$ for a single exponential decay without any stretching.*

each region of the sample has the same stretched relaxation function (this would be dynamical homogeneity). The two cases are depicted schematically in Fig. 6.

The question can be decided by experiment. The most important technique to do so is NMR, but there are several other possibilities. A review of these techniques and their results has been given by Ranko Richert [28]. It turns out that one has indeed dynamical heterogeneity, at least in the sense that the relaxation functions of different regions in the sample have largely different average relaxation times. Again, we return to the question in the section on new developements.

In most cases, the measurement of the stretching is done in the frequency domain. One can, for example, apply a small-amplitude sinusoidal shear strain $\epsilon_s(t) = \epsilon_0 \cos(\omega t)$ to the sample. Then one needs to exert a sinusoidal shear stress

$$\sigma_s(t) = G'(\omega)\epsilon_0 \cos(\omega t) + G''(\omega)\epsilon_0 \sin(\omega t). \tag{12}$$

$G'(\omega)$ and $G''(\omega)$ are the real and imaginary parts of the complex frequency-dependent shear modulus. $G''(\omega)$, the out-of-phase part of the response, is a measure for the loss at the frequency ω.

Fig. 7 shows the real and imaginary part of the complex shear modulus of glycerol [29] slightly above the glass transition. The comparison with the dashed curve for a single exponential clearly shows a sizable stretching. Glycerol is a Type-A glass former (one distinguishes Type-A = no visible secondary relation peak and Type-B = clearly visible secondary relaxation peak), but one can naturally imagine a small secondary relaxation peak hidden in the extended high-frequency tail. We return to this question in section 4 on new developments.

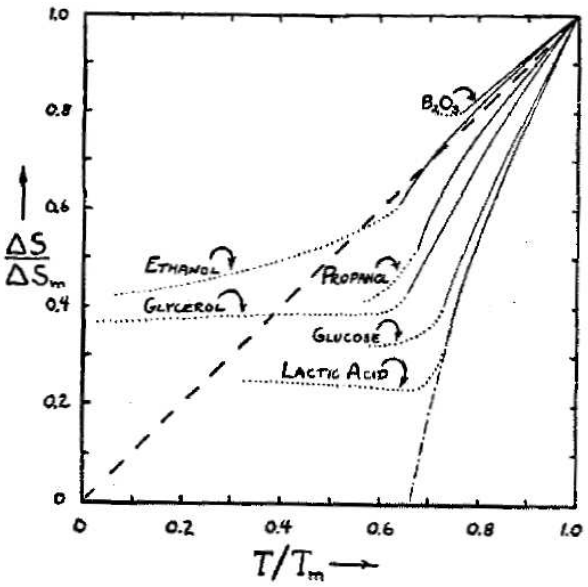

Fig. 8: *Kauzmann's [30] original picture of the loss of the excess entropy $\Delta S = S_{liquid} - S_{crystal}$ on cooling down from the melting temperature in several glass formers.*

3 Thermodynamics of the glass transition

3.1 The Kauzmann catastrophe

Once one is well below the glass transition, the thermodynamics of the glass is rather similar to the one of the crystal. In the example of selenium, the heat capacity c_p of both crystal and glass is close to the classical Dulong-Petit-value of $3k_B$ per atom, due to the three vibrations per atom.

In the undercooled liquid, one has not only the fast energy fluctuations of the vibrations on the picosecond scale, but also the slow energy fluctuations of the structural rearrangements at the relaxation time τ_α. This leads to an additional heat capacity Δc_p. This Δc_p has values between 0.1 and 2 k_B per atom, depending on the specific glass former [6].

Since the heat capacity of the undercooled liquid is higher than the one of the crystal, the undercooled liquid gradually looses the excess entropy $\Delta S = S_{liquid} - S_{crystal}$ over the crystal on cooling. At the melting temperature T_m, $\Delta S = S_m = \Delta H_m/T_m$, where ΔH_m is the latent heat of melting. The melting entropy (which is the physical reason for melting, because it makes the free energy of the liquid more favorable at higher temperatures) is of the order of 0.5 k_B per atom, implying the possibility of about two structural choices per atom in the liquid state. If Δc_p is large, the undercooled liquid rapidly looses this excess entropy on cooling. A linear extrapolation allows to determine the so-called Kauzmann temperature T_K, defined by Kauzmann [30] back in 1948. At the Kauzmann temperature, the entropy of liquid and crystal would be equal, implying essentially only one single possible structural realization of the liquid. It is clear that, at this temperature, the viscosity must diverge, because the liquid becomes unable to jump from one structural realization to another. Fig. 8 shows the Kauzmann extrapolation for some glass formers from his original paper [30]. The figure shows that the glass transition occurs before the undercooled liquid looses all its excess entropy. Thus the "Kauzmann catastrophe" (a liquid with less than one structural configuration) is avoided.

But one can compare the Vogel-Fulcher temperature T_0 (the temperature where the viscosity

would diverge) with the Kauzmann temperature T_K. A comparison to 54 glass formers [26] showed good general agreement, but with four glass formers where T_0 was decidedly smaller than T_K, out of the error bars. Nevertheless, most scientists in the field feel convinced that there is indeed a true physical connection between viscosity and excess entropy. This conviction is further supported by the success of the Adam-Gibbs conjecture [31]

$$\tau_\alpha = \tau_0 \exp\left(\frac{C}{T\Delta S}\right), \tag{13}$$

where C is a constant. The Adam-Gibbs scheme links τ_α and excess entropy via a model of cooperatively rearranging regions, the size of which diverges at the Kauzmann temperature. For a linear dependence of ΔS on temperature, it leads again to the Vogel-Fulcher relation (10) with $T_0 = T_K$.

3.2 The Prigogine-Defay ratio

The question of the nature of the slow structural rearrangements in the undercooled liquid is intimately related to a thermodynamic puzzle, the Prigogine-Defay ratio of the glass transition [32]

$$\Pi = \frac{\Delta c_p \Delta\kappa}{(\Delta\alpha)^2 T_g} = \frac{\overline{\Delta H^2}\ \overline{\Delta V^2}}{(\overline{\Delta H \Delta V})^2}, \tag{14}$$

which relates the increases of the heat capacity per volume unit Δc_p, of the compressibility $\Delta\kappa$ and of the thermal volume expansion $\Delta\alpha$ at the glass temperature T_g to the structural rearrangement enthalpy and volume fluctuations ΔH and ΔV, respectively. If the enthalpy and volume fluctuations are completely correlated, the Prigogine-Defay ratio is one. It has been argued that this is the physically simple case from which one should try to understand the glass transition [33, 34]. We will come back to this proposal in section 4 on new developments.

The Prigogine-Defay ratio is found to be exactly 1 at second order phase transitions (a derivation on the basis of the two Ehrenfest relations for the pressure dependence of the transition temperature is given in Appendix A). A second order phase transition is characterized by continuous first derivations of the enthalpy H, so the volume V and the entropy S are continuous (unlike the first order melting transition, where entropy and volume of liquid and crystal at the melting point are different). At the glass transition, the entropy and the volume are indeed continuous; nevertheless, it is not a second order phase transition, because one of the two phases - the glass - is not in thermal equilibrium. Thus one cannot wonder that real glass formers show Prigogine-Defay ratios much larger than 1 at their glass transition (see Table I). As a rule, stronger glasses have a higher Prigogine-Defay ratio than fragile ones.

subst.	SiO_2	GeO_2	B_2O_3	glycerol	Se	PS	BPA-PC
Π	>100	6.85	4.7	3.7	1.85	1.3	1.02
m	20	20	32	53	87	139	132

Table 1: *Measured Prigogine-Defay ratios of seven glass formers at their glass transition [34, 35]. The fragility m is taken from the collection of Böhmer, Ngai, Angell and Plazek [27].*

4 New developments

4.1 Numerical simulations

The most important new development in the field is the application of numerical methods to the glass transition. One can nowadays study the time development of up to hundred thousand interacting particles on the computer. The technique is called "molecular dynamics" and involves the calculation of the motion of the particles in short time steps, short enough to linearize the particle motion. This implies times steps much shorter than one period of the fast vibrations, in real substances of the order of femtoseconds. With a femtosecond, one has to make a million time steps to arrive at a nanosecond. This limits the method at present to relaxation times which are shorter than a microsecond. As a consequence, one cannot study the glass formers in thermal equilibrium at lower temperatures, where τ_α exceeds a microsecond. One just gets slightly below the critical temperature T_c of the mode coupling theory. Thus the first applications of the method have been to test and to verify the mode coupling theory [36, 37]. Later, it has been used to verify a deep and surprising connection [9] between the mode coupling theory and spin glass theory [4], which will be discussed in the next paragraph on new theoretical developments.
In the calculations, one puts the particles in a cubic box with periodic boundary conditions. A particle is free to leave the box (entering the box from the opposite side) and interacts with the particles in the neighboring boxes. The time needed to calculate all particle interactions increases drastically with the range of the potential. Therefore one prefers short-range anharmonic potentials like the Lennard-Jones potential

$$V(r) = 4\epsilon \left[\left(\frac{\sigma}{r}\right)^{12} - \left(\frac{\sigma}{r}\right)^{6} \right], \tag{15}$$

where r is the interparticle distance, ϵ is the depth of the potential well and σ is close to the resulting nearest-neighbor distance (the potential minimum is at $\sigma/2^{1/6}$).
If one just takes the simple Lennard-Jones potential, one finds crystallization to an fcc structure even for the short simulation times. In order to avoid crystallization, it turns out to be necessary to use binary mixtures of particles with different σ. The most popular of these mixtures is the binary Lennard-Jones mixture introduced by Kob and Andersen [36].
With numerical simulations, one can attack the unsolved problems of the glass transition, for instance the question of the Prigogine-Defay ratio. This has been done for the simple Lennard-Jones system [33], calculating not the Prigogine-Defay ratio, but rather the correlation between the enthalpy H and the volume V

$$\Pi^{-1/2} = \frac{\overline{HV}}{\sqrt{\overline{H^2}\;\overline{V^2}}}, \tag{16}$$

a correlation which involves not only the slow structural degrees of freedom, but the fast vibrations as well.
It is easier to do this in a constant volume calculation at constant temperature (the NVT ensemble), looking at the correlation between pressure fluctuations and energy fluctuations. In this calculation, one has to subtract the ideal gas term, because the pressure p is given by

$$pV = Nk_BT + W, \tag{17}$$

where only the second term, the virial W, is due to the interatomic potential. As one can see in Fig. 9, the virial is indeed highly correlated with the potential energy, with a correlation factor

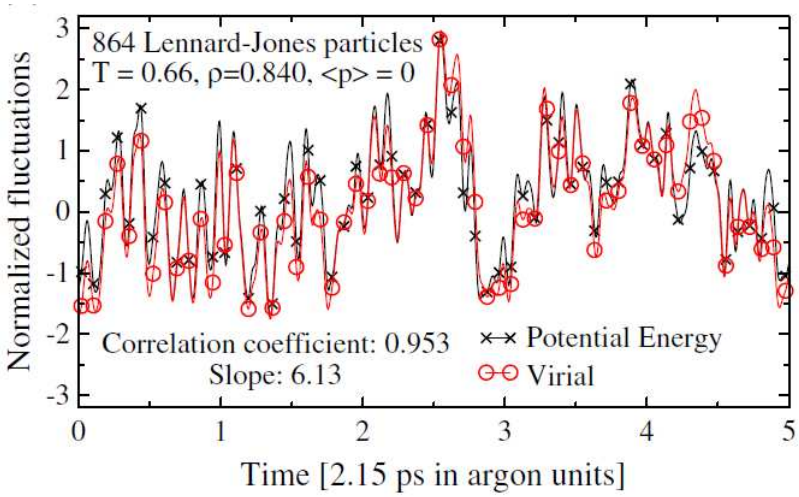

Fig. 9: *Instantaneous normalized equilibrium fluctuations of virial W and potential energy U in the standard single-component LennardJones (LJ) liquid at constant volume (NVT simulation), showing that W(t) and U(t) correlate strongly [33].*

0.953 corresponding to a Prigogine-Defay ratio of 1.1. The same high correlation is found in all simulations of Van der Waals and metallic liquids, but not in hydrogen-bonded liquids like water and glycerol.

On the basis of these results, it has been argued that a Prigogine-Defay ratio of 1 is the physically simple case from which one should try to understand the glass transition [33, 34]. But this is opposed to the arguments in the introduction of the present paper, which indicate that the physically simple case is a harmonic glass former. In a harmonic glass former, the thermal expansion should be zero. Therefore the linear correlation $\overline{\Delta H \Delta V}$ should be zero; the Prigogine-Defay ratio should be infinity (as one indeed finds in silica [38] with $\Pi > 100$).

What brings the Prigogine-Defay ratio down, is the anharmonicity of the potential, which also causes the thermal expansion. With anharmonicity, even a pure shear energy fluctuation is accompanied by a volume fluctuation. If these additional volume fluctuations dominate, the Prigogine-Defay ratio goes to one. In numerical work [36, 33], one usually prefers anharmonic potentials, which vanish at a relative close distance from the atoms. Thus one tends to conclude that the deviation of the Prigogine-Defay ratio from one is an indication for a complicated atomic potential [33, 34]. But it is rather an indication for a harmonic atomic potential.

This point of view is supported by Fig. 10, taken from a very recent paper [40]. As a measure for the anharmonicity at the glass temperature T_g, one can use the product $\alpha_l T_g$, where α_l is the volume expansion coefficient of the liquid. Fig. 10 shows the correlation coefficient $\Pi^{-1/2}$ as a function of this product. Though again the experimental data [34, 35] scatter strongly, one finds clear evidence for a linear increase at low anharmonicity. The simulation value for the zero-pressure binary Kob-Andersen mixture [33] corresponds to rather high anharmonicity.

Fig. 10 demonstrates the limitations of numerical simulations: They do not get very low in temperature and they tempt scientists to overestimate the importance of anharmonic potentials. In spite of these limitations, numerical simulations were at the very bottom of the astonishing progress in the understanding of the glass transition within the last decade, which will be described in the next paragraph.

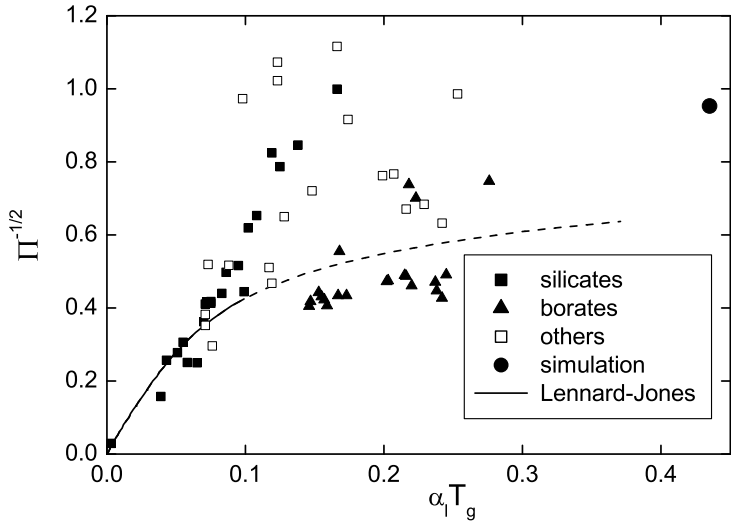

Fig. 10: *The correlation coefficient* $\Pi^{-1/2}$ *(*Π *Prigogine-Defay ratio) as a function of the anharmonicity* $\alpha_l T_g$ *(*α_l *volume expansion coefficient of the liquid,* T_g *glass temperature) for 55 glass formers [34, 35, 39] and the binary Kob-Andersen mixture [33]. The line is a numerical calculation for the Lennard-Jones potential in ref. [40], from which the figure was taken.*

4.2 Theoretical developments

The most important theoretical development of the last decade was the discovery of a deep analogy between mode coupling theory [3] and spin glass theory [4]. There is an excellent recent review of the topic [9], which demonstrates the intimate connection between theory and numerical simulation in this development.

The merit of the mode coupling theory [3] is not so much its prediction of a divergence of the viscosity at T_c - the viscosity does not really diverge there, because thermally activated processes take over - but its prediction of a slowing down of the flow relaxation time τ_α from the vibrational picosecond time scale as one lowers the temperature towards T_c. According to the mode coupling theory, this separation of time scales occurs *without* any activated process. As one approaches T_c, the structural correlation functions decay in two steps, the first in the picosecond regime and the second at τ_α.

However, since the mathematical apparatus of the mode coupling theory is rather complicated, it is not easy to assess a clear physical significance to the separation of time scales. It was said that τ_α corresponded to the "breaking of the cage of neighboring particles", but this is not much more than a figure of speech.

A much deeper explanation became possible when it was realized that the dynamic mode coupling equations are the same as those for the mean field p-spin model [41], a spin-glass model with the Hamiltonian

$$H = -\Sigma_{i,j,k=1}^{N} J_{ijk}\sigma_i\sigma_j\sigma_k \tag{18}$$

for $p = 3$, where J_{ijk} are frozen random variables and σ_i, σ_j and σ_k are spin variables. Since each spin interacts which each pair of other spins irrespective of their distance, the model contains no space information.

The advantage of the p-spin model is that it allows to calculate all important properties. Thus one can analyze what happens as one approaches T_c. One finds [42] that the separation of times scales is due to the properties of the saddle points of the system, which have the tendency to

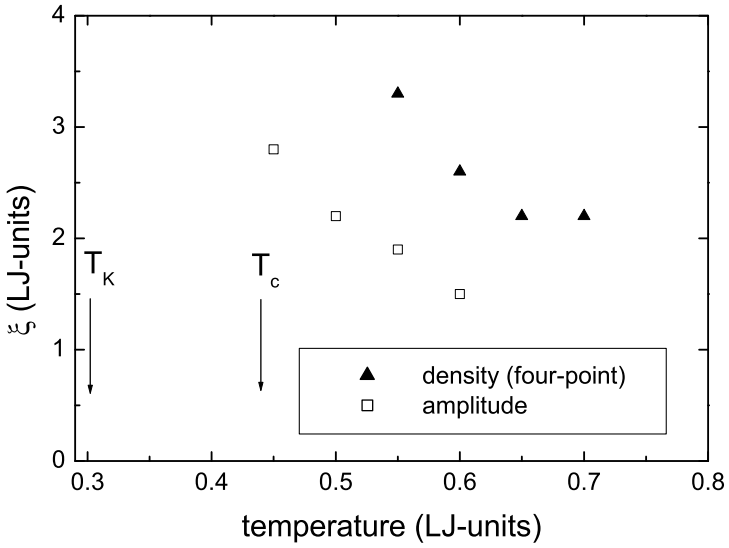

Fig. 11: *Simulation results for a diverging length scale in the binary Kob-Andersen Lennard-Jones mixture from the 4-point correlation function [45] and from the amplitude correlation in shear-induced inherent structure changes [46].*

become isolated true free energy minima toward T_c. This makes the way between two given equilibrium configuration of the system longer and longer as one approaches T_c. Thus the separation of time scales predicted by the mode coupling theory can be identified quantitatively as a phase space property [9].

Scarcely less important, the replica technique (sometimes also called "cloning theory") developed in the context of spin glass theory [4] allows to do calculations for the undercooled liquid below T_c. Thus one calculate the heat capacity [43] for a given interatomic potential between T_c and the Kauzmann temperature T_k. Similarly, one finds the temperature dependence of the plateau shear modulus G_{high} between these two temperatures [15], concluding that it decreases to zero as one reaches T_c.

Again in the same context, the spin glass ideas have been extended to structural glasses in an intense search for a dynamic length scale [44, 45, 46] which is supposed to diverge at the Kauzmann temperature T_k. There is increasing numerical evidence [45, 46] (see Fig. 11) for such a diverging length scale in the binary Kob-Andersen Lennard-Jones mixture, supporting the Adam-Gibbs concept [31] of cooperatively rearranging regions. The motivation of the work is to clarify the deep connection between thermodynamics and dynamics reflected in the validity of the Adam-Gibbs equation (13).

A theoretical scheme which indeed leads to a validity of the Adam-Gibbs equation is the mosaic theory or random-first-order theory [47] (RFOT), motivated by the parallel between mode coupling theory and spin glass models. According to RFOT, the diameter of a cooperatively rearranging region results from the thermodynamic equilibrium between the entropy inside the region and the surface tension at the interface to neighboring regions. One has to postulate a surface tension coefficient which depends on the diameter to get the Adam-Gibbs equation, but one can find a theoretical justification for this [47].

The theoretical evolution described so far seems fairly coherent and convincing, but there are other and independent theoretical attempts to understand the glass transition. Some of them are described at the end of Cavagna's excellent review [9]. Others are motivated by new experi-

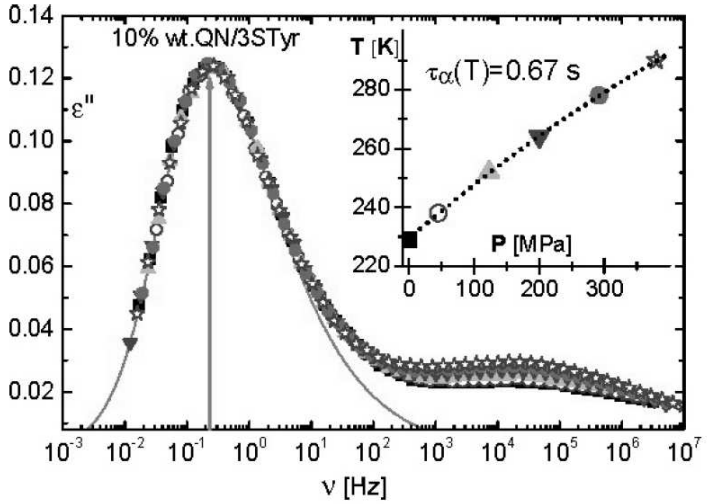

Fig. 12: *Dielectric spectra of 10 mol%-quinaldine in tristyrene at different pressures and adapted temperatures [48]. The inset shows the curve in the temperature-pressure diagram which must be followed to keep the primary peak frequency at the same place.*

mental findings and will be described in the next paragraph.

4.3 New experimental findings

Though a bit overshadowed by the success of the numerical simulations described above, the progress in experimental techniques for the study of the glass transition is by no means contemptible. The main progress has been made by the development of broadband dielectric spectroscopy [49, 50]. It is nowadays possible to measure the dielectric spectrum from 10^{-6} to 10^{12} Hz (though the GHz region is still not easy to measure). Even more important, one can measure the dielectric spectrum under high pressure. If one does this for glycerol, which has no clearly visible secondary relaxation at ambient pressure, one does indeed see the development of a clear secondary peak [51].

Fig. 12 shows a measurement of a binary mixture, 10-mol% of quinaldine in tristyrene [48]. One sees the large and broad α- peak at low frequency and a smaller secondary peak at higher frequency. This is a clever pressure experiment, varying temperature and pressure simultaneously in such a way that the primary peak stays at the same frequency. One finds the striking result that the secondary peak also stays at the same place, indicating a connection between α and β-process.

However, the picture can also be quite different [52]. In some systems, where the molecules are not rigid and the secondary relaxation is due to to a molecular configuration change, the primary peak is much more sensitive to pressure than the secondary peak. So it is necessary to distinguish these two cases. If one has a molecular configuration change, the two inherent states which contribute to the secondary relaxation will be separated by a practically temperature- and pressure-independent barrier. In the other case, one has a barrier between two different molecular arrangements, which will vary with temperature and pressure according to the variation of the elastic constants, in particular the high frequency shear modulus G_{high} (in fact, the elastic models [10] explain the fragility by a proportionality of the strongly temperature-dependent G_{high} to the flow barrier).

Taking the pressure dependence as an indicator whether one deals with an intramolecular or

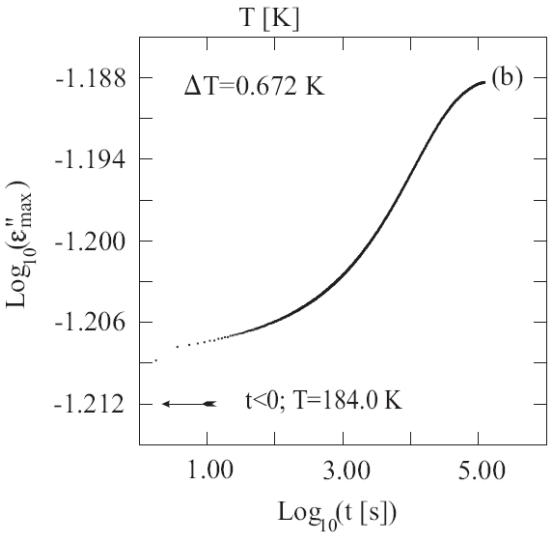

Fig. 13: *Beta loss peak maximum in tripropylene glycol, monitored after a temperature increase of 0.672 K starting from equilibrium at 184.0 K. After 6 s temperature is stable within 1 mK of the final temperature. At this time, the energy landscape has not yet changed, but the peak maximum nevertheless shows already a clearly measurable increase compared to the value before heating, denoted by the arrow [55].*

intermolecular relaxation, one finds [48, 52, 53] that the relaxation time τ_β of the latter ones always follows the coupling model relation [53]

$$\tau_\beta = \tau_\alpha^{1-n} t_c^n, \tag{19}$$

where $1-n$ is the Kohlrausch exponent of the primary process and t_c is a short time of the order of 2 ps. According to the coupling model, the α-process reflects the result of the interaction of the "primitive" relaxations in the β-process. This is a picture of the glass transition which is completely different from the mode-coupling and spin-glass concept described in the preceding two paragraphs, but there are many dielectric experiments supporting it [11].
In fact, a connection between α- and β-process has been demonstrated directly in another key experiment [54], done by NMR on sorbitol. This experiment is one of the many measurements demonstrating dynamical heterogeneity [28], i.e. different relaxation times at different places in the sample. The NMR technique can be used to separate subensembles of the sample which belong to a specific relaxation time. The experiment showed that a subensemble which has a slow α-relaxation time also tends to have a slow β-relaxation time. As the authors [54] point out, there is at present only a single theoretical explanation for such a behavior, namely Kia Ngai's coupling model [53].
The last experiment reported here is a unique aging experiment [55] close to the glass temperature, where the relaxation time τ_α is of the order of a day. It is done within a sample holder for dielectric measurements which is able to change the temperature to a new equilibrium within a few seconds. This allows to see what happens with the fast secondary relaxation during the aging process.
Fig. 13 shows the development of the amplitude of the secondary process in tripropylene glycol at 184 K, where the primary process has a relaxation time of a day. After a quick heating to the temperature 184.672 K, one follows the gradual approach to equilibrium at long times.

But the surprising thing is: One already sees a small, but decidedly measurable increase of the amplitude at short times, after the equilibration time of the temperature. This means an increase within an unchanged energy landscape, and this in turn has only one possible explanation: The inherent states, between which the system jumps back and forth in the secondary relaxation, must be strongly asymmetric. One can calculate the average asymmetry from the increase. For the one in Fig. 12, one finds an average asymmetry of 3.8 $k_B T_g$, a factor four or more larger than one would expect.

This is not a specific property of tripropylene glycol, because the authors measured it in several systems, including a toluene-pyridine mixture of rigid molecules. It seems to be a general phenomenon, irrespective of whether the secondary peak is a molecular rearrangement of rigid molecules or an intra-molecular configuration change.

An explanation of this asymmetry was proposed by the author [56] in terms of the Eshelby backstress [2]. If the system searches for possible neighboring inherent states, it will most probably find a mayority of elastically distorted states, which do not fit well into the present strain of the surrounding matrix. The concept allows to predict an asymmetry of 4 $k_B T$ without any adaptable parameter, close to the observed value in tripropylene glycol.

If this hypothesis is generally true, the α-relaxation should show the same asymmetry. Some of the implications of such a general asymmetry have been worked out in a series of papers [40, 56, 57].

5 Summary

The glass transition is at present a very active field of research. The main reason for this is the very fruitful cooperation of theory and numerical simulation described in Section 4 of this paper [9]. It encourages the hope for a closed quantitative and convincing description of the glass transition within the next decade. In this description, there is a separation of time scales on cooling the undercooled liquid, which occurs when the valleys in the free energy landscape are no longer connected. The onset of this separation of time scales is well described by the mode coupling theory [3]. As one approaches the critical temperature of the mode coupling theory from above, thermally activated hopping between the minima of the free energy landscape (at this temperature already practically the potential energy landscape [5, 7]) sets in. In this temperature regime, the glass formers approach a true thermodynamic second order transition at the Kauzmann temperature. The more fragile the glass former is, the closer it gets to the Kauzmann temperature. In this regime, one can calculate physical properties quantitatively if one knows the interatomic potentials, using the replica or cloning theory [15, 43].

On the other hand, there are important experimental facts which remain unexplained and are not (or not yet) integrated into this appealing picture: the role of the anharmonicity [40], the relations between primary and secondary relaxation processes which seem to be well described by the coupling model [11] and the asymmetry of the secondary relaxation [55], which can be argued [56] to be a general property due to the Eshelby backstress [2].

Appendices

A The Prigogine-Defay ratio at a second order phase transition

The differential of the Gibbs free energy G is given by

$$dG = -SdT - Vdp, \tag{20}$$

where S is the entropy, T the temperature, V the volume and p the pressure of the system. From this equation follows the Maxwell relation

$$\frac{\partial^2 G}{\partial T \partial p} = -\left(\frac{\partial S}{\partial p}\right)_T = \left(\frac{\partial V}{\partial T}\right)_p = -V\alpha, \tag{21}$$

where α is the thermal expansion, because the order of the two diffentiations of G is irrelevant. Now consider a second order phase transition between phases A and B, in which entropy and volume are continuous. The two phases join at the transition temperature $T_c(p)$, which depends on the pressure and thus yields a transition line in a p, T-diagram. Along this line, one has two continuity relations, the first from the entropy

$$\left(\frac{\partial S_A}{\partial T}\right)_p dT + \left(\frac{\partial S_A}{\partial p}\right)_T dp = \left(\frac{\partial S_B}{\partial T}\right)_p dT + \left(\frac{\partial S_B}{\partial p}\right)_T dp \tag{22}$$

and the second from the volume

$$\left(\frac{\partial V_A}{\partial T}\right)_p dT + \left(\frac{\partial V_A}{\partial p}\right)_T dp = \left(\frac{\partial V_B}{\partial T}\right)_p dT + \left(\frac{\partial V_B}{\partial p}\right)_T dp. \tag{23}$$

The derivatives of S with respect to p can be replaced by the Maxwell relation (21). $(1/V)\partial S/\partial T$ at constant pressure is the heat capacity c_p per volume unit, $-(1/V)\partial V/\partial p$ at constant temperature is the isothermal compressibility κ_T. With these definitions, and setting Δc_p, $\Delta\alpha$ and $\Delta\kappa_T$ for the differences of phase A and phase B in heat capacity, thermal expansion and compressibility, respectively, one obtains the two Ehrenfest relations

$$\frac{\partial T_c}{\partial p} = \frac{T\Delta\alpha}{\Delta c_p} \tag{24}$$

and

$$\frac{\partial T_c}{\partial p} = \frac{\Delta\kappa_T}{\Delta\alpha}. \tag{25}$$

Equating these two, one finds that the Prigogine-Defay ratio of eq. (14) is indeed 1. However, as pointed out above, this equality requires thermal equilibrium in both phases A and B. For the glass transition, one can argue [9] that one reaches this requirement for $T_g = T_K$, which in turn helps to understand why the Prigogine-Defay ratio is indeed close to 1 for very fragile glass formers (see Table I).

References

[1] C. Kittel, *Introduction to Solid State Physics*, 3rd ed., (Wiley, New York 1966), p. 183. This reference does not say anything about the glass transition, but explains the anharmonicity mechanism of the thermal expansion.

[2] J. D. Eshelby, Proc. Roy. Soc. **A241**, 376 (1957). Again, this reference says nothing about the glass transition, but gives the elasticity theory description of a structural rearrangement within an isotropic elastic solid.

[3] W. Götze and S. Sjögren, Rep. Prog. Phys. **55**, 241 (1992). This reference explains the mode coupling theory.

[4] M. Mezard, G. Parisi and M.A. Virasoro, *Spin-Glass theory and beyond* (World Scientific, Singapore, 1987)

[5] M. Goldstein, J. Chem. Phys. **51**, 3728 (1969). The energy landscape concept.

[6] C. A. Angell, W. Sichina, Ann. New York Acad. Sci. **279**, 53 (1976). Experimental results at the glass transition.

[7] P. G. Debenedetti and F. H. Stillinger, Nature **410**, 259 (2001). The concept of inherent structures.

[8] F. Leonforte, R. Boissiere, A. Tanguy, J. P. Wittmer and J.-L. Barrat, Phys. Rev. B **72**, 224206 (2005). Nonaffine atomic motion after an affine shear deformation of an amorphous solid.

[9] A. Cavagna, Phys. Rep. **476**, 51 (2009). Review of (a) the connection between mode coupling theory and spin glass theory (b) thermodynamic calculations below the critical temperature of the mode coupling theory with the help of the spin glass theory.

[10] J. C. Dyre, Rev. Mod. Phys. **78**, 953 (2006). A review of the elastic models.

[11] K. L. Ngai, *Relaxation and Diffusion in Complex Systems* (Springer, Berlin 2011). Describes the experimental evidence for the coupling model.

[12] U. Buchenau, J. Non-Cryst. Solids **357**, 274 (2011). Key experiments in highly viscous liquids.

[13] S. V. Nemilov, *Thermodynamic and Kinetic Aspects of the Vitreous State*, (CRC Press, Ann Arbor 1995)

[14] E. Donth, *The Glass Transition*, (Springer, Berlin 2001)

[15] H. Yoshino and M. Mezard, Phys. Rev. Lett. **105**, 015504 (2010)

[16] U. Buchenau and R. Zorn, Europhys. Lett. **18**, 523 (1992)

[17] J. Wuttke, W. Petry, G. Coddens and F. Fujara, Phys. Rev. E **52**, 4026 (1995)

[18] F. Scarponi, L. Comez, D. Fioretto and L. Palmieri, Phys. Rev. B **70**, 054203 (2004)

[19] U. Buchenau, Yu. M. Galperin, V. L. Gurevich, D. A. Parshin, M. A. Ramos and H. R. Schober, Phys. Rev. B **46**, 2798 (1992)

[20] H. G. E. Hentschel,S. Karmakar, E. Lerner and I. Procaccia, Phys. Rev. E **83**, 061101 (2011)

[21] W. Schirmacher, G. Ruocco and T. Scopigno, Phys. Rev. Lett.**98**, 025501 (2007)

[22] W. A. Phillips, U. Buchenau, N. Nücker, A. J. Dianoux and W. Petry, Phys. Rev. Lett. **63**, 2381 (1989)

[23] A. Wischnewski, U. Buchenau, A. J. Dianoux, W. A. Kamitakahara, and J. L. Zarestky, Phys. Rev. B **57**, 2663 (1998)

[24] A. Reiser, Ph. D. thesis, Univ. Heidelberg 2005

[25] C. A. Angell, Science **267**, 1924 (1995)

[26] L.-M. Wang, C. A. Angell and R. Richert, J. Chem. Phys. **125**, 074505 (2006)

[27] R. Böhmer, K. L. Ngai, C. A. Angell and D. J. Plazek, J. Chem. Phys. **99**, 4201 (1993)

[28] R. Richert, J. Phys.: Condens. Matter **14**, R703 (2002)

[29] K. Schröter and E. Donth, J. Chem. Phys. **113**, 9101 (2000)

[30] A. W. Kauzmann, Chem. Rev. **43**, 219 (1948)

[31] G. Adam and J. H. Gibbs, J. Chem. Phys. **43**, 139 (1958)

[32] J. Jäckle, J. Chem. Phys. **79**, 4463 (1983)

[33] U. R. Pedersen, N. Gnan, N. P. Bailey, T. B. Schroeder and J. C. Dyre, J. Non-Cryst. Solids **357**, 320 (2011)

[34] D. Gundermann, U. R. Pedersen, T. Hecksher, N. P. Bailey, B. Jakobsen, T. Christensen, N. B. Olsen, T. B. Schroeder, D. Fragiadakis, R. Casalini, C. M. Roland, J. C. Dyre and K. Niss, Nature Physics **7**, 816 (2011)

[35] D. B. Dingwell, R. Knoche and S. L. Webb, Phys. Chem. Minerals **19**, 445 (1993)

[36] W. Kob and H.C. Andersen, Phys. Rev. E **52**, 4134 (1995)

[37] H. R. Schober, Phys. Rev. Lett. **88**, 145901 (2002)

[38] D. M. Krol, K. B. Lyons, S. A. Brawer and C. R. Kurkjian, Phys. Rev. B **33**, 4196 (1986)

[39] S. V. Nemilov, V. N. Bogdanov, A. M. Nikonov, S. N. Smerdin, A. I. Nedbai and B. F. Borisov, Fiz. i Khim. Stekla **13**, 801 (1987) (Sov. J. Glass Phys. Chem. **13**, 413 (1987))

[40] U. Buchenau, arXiv:1110.5066 (cond-mat:dis-nn]

[41] J.-P. Bouchaud, L. Cugliandolo, J. Kurchan and M. Mezard, Physica A **226**, 243 (1996)

[42] A. Cavagna, I. Giardina and G. Parisi, Phys. Rev. B **57**, 11251 (1998)

[43] M. Mezard and G. Parisi, J. Phys. A: Math. Gen. **29**, 6515 (1996)

[44] L. Berthier, G. Biroli, J. P. Bouchaud, W. Kob, K. Miyazaki and D. R. Reichman, J. Chem. Phys. **126**, 184503 (2007)

[45] S. Karmakar, C. Dasgupta and S. Sastry, Phys. Rev. Lett. **105**, 015701 (2010)

[46] M. Mosayebi, E. Del Gado, P. Ilg and H. C. Öttinger, Phys. Rev. Lett. **104**, 205704 (2010)

[47] T.R. Kirkpatrick, D. Thirumalai and P.G. Wolynes, Phys. Rev. A **40**, 1045 (1989)

[48] K. Kessairi, S. Capaccioli, D. Prevosto, M. Lucchesi, S. Sharifi, and P. A. Rolla, J. Phys. Chem. B **112**, 4470 (2008)

[49] U. Schneider, P. Lunkenheimer, R. Brand and A. Loidl, J. Non-Cryst. Solids **235-237**, 173 (1998)

[50] *Broadband dielectric Spectroscopy*, ed. F. Kremer and A. Schönhals (Springer, Berlin, 2002)

[51] A. A. Pronin, M. V. Kondrin, A. G. Lyapin, V. V. Brazhkin, A. A. Volkov, P. Lunkenheimer and A. Loidl, Phys. Rev. E **81**, 041503 (2010)

[52] K. L. Ngai and M. Paluch, J. Chem. Phys. **120**, 857 (2004)

[53] K. L. Ngai, Comments Solid State Phys. **9**, 121 (1979); J. Phys.: Condens. Matter **15**, 1107 (2003)

[54] R. Böhmer, G. Diezemann, B. Geil, G. Hinze, A. Nowaczyk and M. Winterlich, Phys. Rev. Lett. **97**, 135701 (2006)

[55] J. C. Dyre and N. B. Olsen, Phys. Rev. Lett. **91**, 155703 (2003)

[56] U. Buchenau, J. Chem. Phys. **131**, 074501 (2009)

[57] U. Buchenau, J. Chem. Phys. **134**, 224501 (2011)